

35. Variants of Solid-State and Solution Structures of (η^3 -Allyl)- {2-[2'-(diphenylphosphino)phenyl]-4,5-dihydrooxazole-*P,N*}palladium(II) Hexafluorophosphates and Tetraphenylborates

by Silvia Schaffner, Ludwig Macko, Markus Neuburger, and Margareta Zehnder*

Institut für Anorganische Chemie der Universität Basel, Spitalstrasse 51, CH-4056 Basel

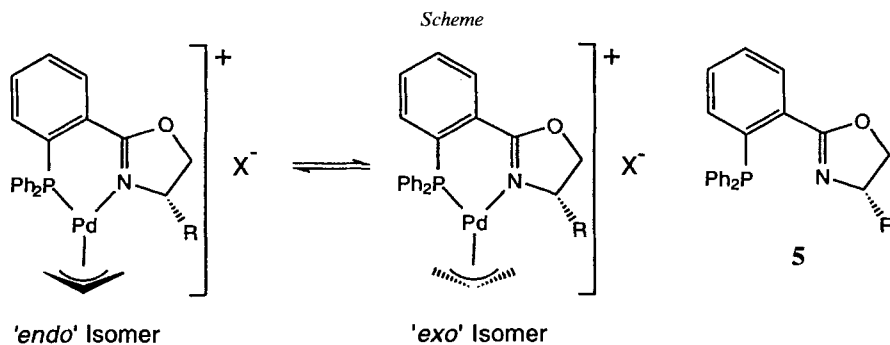
(19.VIII.96)

Crystal and solution structures of the enantiomerically pure and the racemic pairs of (η^3 -allyl){2-[2'-(diphenylphosphino)phenyl]-4,5-dihydro-4-phenyloxazole}palladium(II) hexafluorophosphates (**1**, and *rac-1*, resp.) and tetraphenylborates (**2**, and *rac-2*, resp.) as well as (η^3 -allyl){2-[2'-(diphenylphosphino)phenyl]-4,5-dihydro-4-isopropoxyloxazole}palladium(II) tetraphenylborate (**3**) were characterized by X-ray crystallography and $^1\text{H-NMR}$ spectroscopy. In the solid state, *rac-1* and *rac-2* proved to be disordered with both diastereoisomeric complexes in the crystal. The complexes **2** and **3** exist only in the 'exo' form. The X-ray structures show that the $[\text{Pd}^{\text{II}}(\eta^3\text{-allyl})]$ moiety may adopt different configurations between a nearly symmetrical three-electron $\text{Pd}(\pi\text{-allyl})$ system and an asymmetrical allyl group with a η^1 - and a η^2 -bonding to the metal center. The $[\text{Pd}^{\text{II}}(\eta^3\text{-allyl})]$ system of *rac-1* and of 'endo' *rac-2* is closer to the former, and that of **2**, 'exo'-*rac-2*, and **3** closer to the later geometry. The $^1\text{H-NMR}$ spectra of the hexafluorophosphates **1** and *rac-1* show two sets of signals of the allylic protons in an 'exo'/'endo' ratio of 2:3. The tetraphenylborates **2**, *rac-2*, and **3** give only one set of broad signals of the allylic protons.

Introduction. – Chiral 4-substituted 2-[2'-(diphenylphosphino)phenyl]-4,5-dihydrooxazoles (*Scheme*) induce high yields and excellent enantioselectivities in Pd-catalyzed allylic substitution reactions [1]. In the standard reaction of dimethyl malonate with racemic 1,3-diphenylprop-2-enyl acetate, enantioselectivities of up to 99% were reached [1a]. The relevant intermediates in the catalytic process are the $[\text{Pd}^{\text{II}}(\eta^3\text{-1,3-diphenylallyl})]$ complexes. Here we focus on the structures of the corresponding $[\text{Pd}^{\text{II}}(\eta^3\text{-C}_3\text{H}_5)]$ complexes. These are of interest because the 'endo' and 'exo' isomers of the PF_6^- salts exist in nearly equal amounts in solution and in the crystalline state [2] and can be studied by X-ray analysis (*Scheme*). We have recently found that the equilibrium of the benzyl derivative **4** was not affected by modifying temperature or solvent [3].

To obtain more information on the influence of the counterion on the structures and the 'endo'/'exo' equilibria, we isolated the $[\text{Pd}^{\text{II}}(\eta^3\text{-C}_3\text{H}_5)]$ hexafluorophosphates and tetraphenylborates with 2-[2'-(diphenylphosphino)phenyl]-4,5-dihydro-4-phenyloxazole. The enantiomerically pure complexes **1** and **2**, and the racemic complexes *rac-1* and *rac-2* were investigated (*Scheme*). To assess the influence of the tetraphenylborate anion on the structures of the Pd^{II} complexes, the isopropyl derivative **3** was also included in this study.

Crystal Structures. – The structures of *rac-1*, **2**, *rac-2*, and **3** are determined by X-ray crystallography. Selected geometrical parameters are reported in *Table 1* (for numbering, see *Figs. 1–4*). A superposition of the three phenyl derivatives shows that the essential



1 and *rac-1* R = Ph, X⁻ = PF₆⁻
2 and *rac-2* R = Ph, X⁻ = BPh₄⁻

3 R = *i*-Pr, X⁻ = BPh₄⁻
4 R = PhCH₂, X⁻ = PF₆⁻

Table 1. Selected Parameters [\AA , $^\circ$] with *e.s.d.*'s in Parentheses for *rac-1*, **2**, *rac-2*, and **3**

	<i>rac-1</i>		2	<i>rac-2</i>		3
	'endo' (51%)	'exo' (49%)	'exo'	'endo' (65%)	'exo' (35%)	'exo'
Pd(1)–N(1)	2.073(3)		2.071(6)	2.097(2)		2.084(5)
Pd(1)–P(1)	2.257(1)		2.264(1)	2.262(1)		2.274(1)
N(1)–Pd(1)–P(1)	90.35(9)		88.0(2)	87.06(7)		88.6(1)
Pd(1)–C(100)	2.107(8)	2.107(8)	2.09(1)	2.122(6)	2.08(1)	2.099(7)
Pd(1)–C(200)	2.16(1)	2.14(1)	2.168(7)	2.149(6)	2.24(1)	2.161(6)
Pd(1)–C(300)	2.234(8)	2.226(8)	2.206(8)	2.173(7)	2.37(2)	2.224(5)
C(100)–C(200)	1.377(9)	1.376(9)	1.41(1)	1.41(1)	1.47(2)	1.41(1)
C(200)–C(300)	1.372(9)	1.375(9)	1.36(1)	1.40(1)	1.30(2)	1.333(9)
C(100)–Pd(1)–C(300)	66.2(5)	67.5(6)	67.6(4)	69.4(3)	65.7(6)	67.4(3)
C(300)–Pd(1)–N(1)	105.8(4)	101.1(4)	103.4(3)	106.0(3)	95.6(4)	102.3(2)
C(100)–Pd(1)–P(1)	97.6(4)	100.7(5)	100.9(3)	96.8(2)	110.9(5)	101.3(2)
Pd–N–P/allyl plane	109.6	124.1	117.4	123.0	122.4	120.1

features of the coordinated phosphinooxazole framework described earlier [3] are very similar (*Fig. 5*) [4]. But with respect to the $[\text{Pd}^{\text{II}}(\eta^3\text{-C}_3\text{H}_5)]$ moiety, some differences are found. In *rac-1*, the allyl group is disordered. A refinement of the crystallographic occupancy factors of all allylic atoms reveals an 'endo'/'exo' ratio of 1:1. In both diastereoisomers, a nearly symmetrical allyl group with equal C–C distances within experimental error is found. The Pd–C bond *trans* to P is longer than the analogue bond *cis* to P arising from the different *trans* influence of the N and P donor atoms. This pattern was also found in allyl complexes with ω -(diphenylphosphino)carboxylates [5]. Complex **2** is not disordered. Only the 'exo' isomer exists in the solid state. This is due to lattice forces rather than to stabilization of this diastereoisomer by the tetraphenylborate anion. Calculations reveal that the 'endo' form would lead to very short H...C

distances of 2.09 and 2.13 Å to the Ph substituent of an adjacent cation [4]. In **2**, the allyl group is bound rather asymmetrically to the Pd-atom. The allylic C–C bond *trans* to P is closer to a double and the C–C bond *trans* to N closer to a single bond. Similar features are also found in chloro(dioxaphosphocine-*P*)(η^3 -2-methylallyl)palladium(II) [6]. In contrast to compound **2**, the allyl group of *rac*-**2** is disordered. The displacement parameters of the unsplit allyl group suggested a different situation than in the other examples described. As refinement of disordered groups is always dependent on assumptions, a minimum set of restraints has been included to let reflection data give the answer. The ‘*endo*’ isomer, which is similar to the allyl system found in *rac*-**1**, predominates with *ca.* 65%. The bond lengths C(100) to C(200) of 1.47(2) and C(200) to C(300) of 1.30(2) found in the ‘*exo*’ isomer show a situation similar to compound **2**. The (η^3 -allyl){4,5-dihydro-4-isopropyl-2-{2'-[(1-naphthyl)phenylphosphino]phenyl}oxazole}palladium(II) cation has a similar allyl group with C–C bonds of 1.44 and 1.28 Å, respectively [2a]. In *rac*-**2**, the Pd–C(300) distance is 2.37(2) Å. In all other similar compounds found in the literature as well as in this work, the Pd–C(allyl) distance *trans* to P is *ca.* 2.20 Å. The X-ray analysis of **3** shows an allyl group similar to **2**.

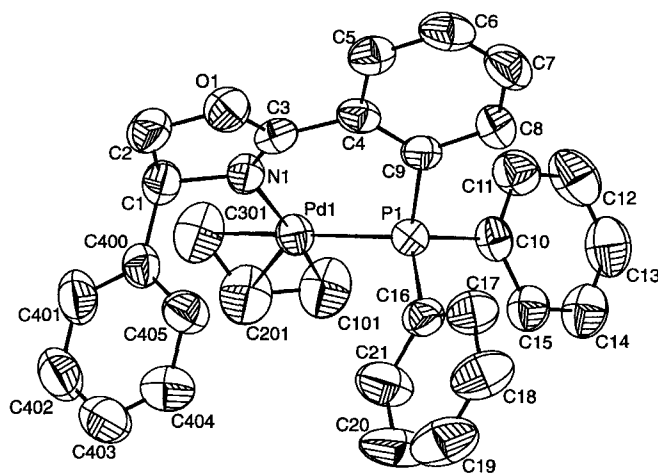


Fig. 1. X-Ray structure of complex *rac*-**1**. Thermal ellipsoids are drawn at 50% probability. Only the ‘*exo*’-allyl is shown.

NMR Spectroscopy. – Selected $^1\text{H-NMR}$ data are summarized in *Table 2*. In CDCl_3 , the identical $^1\text{H-NMR}$ spectra of *rac*-**1** and its chiral analogue **1** show the usual two sets of signals of the allylic protons corresponding to the two diastereoisomers [2][3]. A ratio of *ca.* 3:2 is observed in both compounds. The two sets of signals have been assigned to the two isomers by $^1\text{H-COSY}$ experiments. The major diastereoisomer is assigned to the ‘*endo*’ form, since only the $\text{H}_t\text{-C}(300)^1$ resonance of the ‘*endo*’ isomer is affected by the ring current of the Ph substituent at the oxazole and is shifted to higher field (2.84 ppm) relative to the corresponding signal of the ‘*exo*’ form (3.90 ppm). To a lesser extent, an upfield shift of the signal of the central allylic proton of the ‘*exo*’ isomer is found (5.15

¹) H_t and H_c are the protons in *trans*- and *cis*-position, respectively, to $\text{H-C}(2)$ of the allyl group.

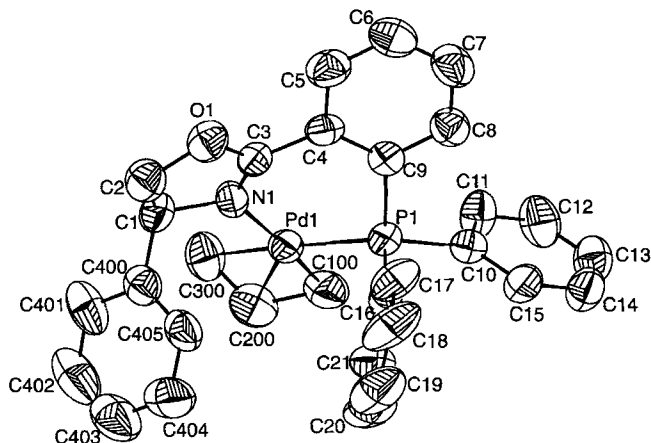


Fig. 2. X-Ray structure of complex **2**. Thermal ellipsoids are drawn at 50% probability.

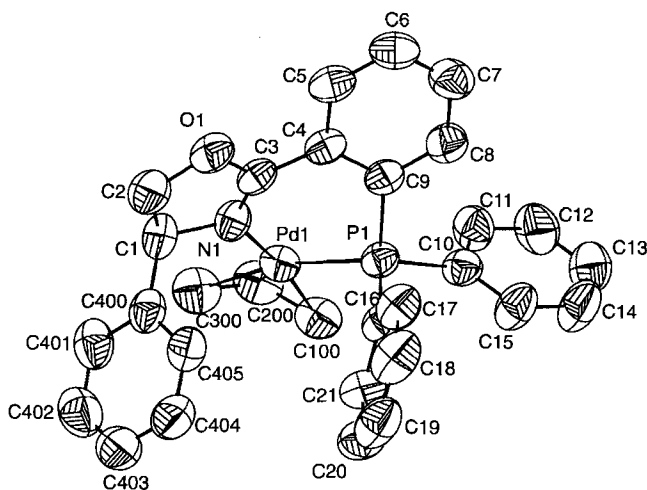


Fig. 3. X-Ray structure of complex *rac-2*. Thermal ellipsoids are drawn at 50% probability. Only the 'endo'-allyl is shown.

vs. 5.62 ppm). Similar shifts are also observed in **4** [3] but not in complexes with aliphatic substituents attached to the dihydrooxazole ring [2]. In all these compounds, the H_t -C(300) chemical shift is > 3.60 ppm and the $H-C(200)$ shift > 5.7 ppm.

The 1H -NMR spectra of **2** and *rac-2* are very similar. In contrast to the PF_6^- salts, they give only one set of signals. The signals of the terminal allylic protons *cis* to P coalesce into a broad peak, which is superimposed onto the H_t -C(300) signal. The central proton shows a badly resolved *m*. 1H -NMR Experiments were also carried out in $CDCl_3$ at -50° . Only one set of very broad allyl resonances is observed. The signals of the protons attached to C(100) are still coalesced, but separated from the broad H_t -C(300) *s*. The signal of H_c -C(300) forms a relatively narrow *s*.

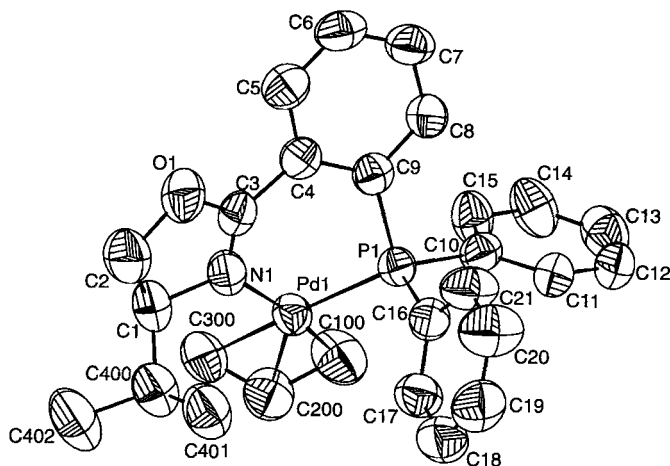


Fig. 4. X-Ray structure of complex 3. Thermal ellipsoids are drawn at 50% probability.

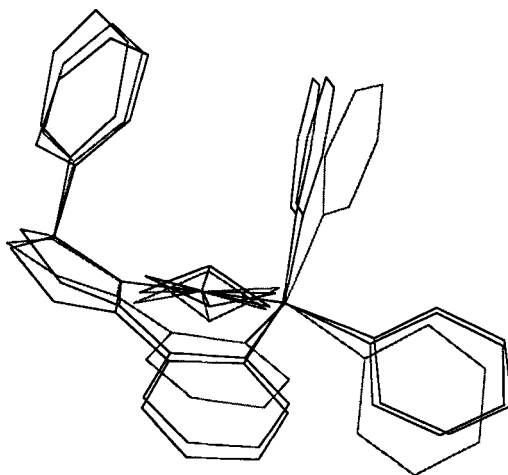


Fig. 5. Superposition of complexes *rac-1* (gray), **2**, and *rac-2*

In **3**, only one set of fairly broad *multiplets* of the allylic protons is found at room temperature. At -50° , both H–C(100) signals form two broad *singlets*. Except for some broadening, the other signals remain unchanged. The broadening may be due to ion association with the anion (see below). The NMR data suggest that BPh_4^- salts exist as a rapidly interconverting mixture of ‘*endo*’ and ‘*exo*’ isomers in solution. This assumption is supported by the fact that in *rac-2*, both isomers exist in the crystal. On the other hand it may not be excluded that the broad signals are due to ion association (see below) and/or decomposition of the complex. Solutions of these compounds become black within a few hours by formation of Pd^0 .

The presence of the BPh_4^- anion gives rise to a significant upfield shift of the signals of the dihydrooxazole and the allylic protons with respect to the PF_6^- salts (Table 3). The

Table 2. Selected $^1\text{H-NMR}$ Data (δ in ppm, J in Hz) of Allyl- and Oxazole Protons in **1**, **2**, and **3** (300 MHz in CDCl_3 at r.t.)

	1 'exo' (40%)	1 'endo' (60%)	2	3
H_t^a -C(100)	2.71 (<i>d</i> , $J = 12.4$)	2.64 (<i>d</i> , $J = 12.1$)	2.7–2.9 (br.) ^d	2.82 (br. <i>d</i>)
H_c^a -C(100)	3.31 (<i>d</i> , $J = 6.1$)	3.18 (<i>d</i> , $J = 6.4$)	2.7–2.9 (br.) ^d	3.15 (br. <i>d</i>)
H–C(200)	5.15 (<i>m</i>)	5.62 (<i>m</i>)	5.11 (<i>m</i>)	5.41 (<i>m</i>)
H_t^a -C(300)	3.90 (<i>dd</i> , $J = 13.3, 9.9^b$)	2.85 (<i>dd</i> , $J = 13.7, 10.2^b$)	2.7–2.9 ^c	3.31 (<i>dd</i> , $J = 10.2, 13.7$)
H_c^a -C(300)	4.49 (<i>m</i>)	4.77 (<i>m</i>)	4.17 (<i>dd</i> , $J = 6.8, 6.8^c$)	4.35 (<i>t</i> , $J = 6.6$)
H_t -C(2)	4.29 (<i>dd</i> , $J = 7.7, 8.8$)		3.96 (<i>dd</i> , $J = 9.1, 8.0$)	4.08 (<i>d</i> , $J = 7.8$)
H_c -C(2)	5.13 (<i>dd</i> , $J = 8.8, 10.5$)		4.40 (<i>dd</i> , $J = 9.1, 10.4$)	4.08 (<i>d</i> , $J = 7.8$)
H–C(1)	5.77 (<i>dd</i> , $J = 7.7, 10.5$)		4.85 (<i>dd</i> , $J = 8.0, 10.4$)	3.90 (<i>dt</i> , $J = 7.8, 3.2$)

^a) H_t : *trans*-configuration, H_c : *cis*-configuration to the central proton.

^b) $J(\text{H}, \text{P})$.

^c) Signal overlap.

^d) Coalescence.

Table 3. Chemical Shifts [ppm] of Allyl and Oxazole Protons of Salt Mixtures (300 MHz in CDCl_3 at r.t.)

mol-% BPh_4^-	Pure 1 (0%)	22%	50%	Pure 2 (100%)	1 → 2 shift
H_t -C(100)	2.96 ^a)	2.94 ^c)	2.90 ^c)	2.8 ^c)	0.16
H_c -C(100)	2.96 ^a)	2.94 ^c)	2.90 ^c)	2.8 ^c)	0.16
H–C(200)	5.39 ^a) ^b)	5.45	5.32	5.11	0.28
H_t -C(300)	3.37 ^a)	3.25	3.08	2.8 ^b)	0.57
H_c -C(300)	4.63 ^a)	4.61	4.46	4.17	0.46
H_t -C(2)	4.29	4.27	4.15	3.96	0.31
H_c -C(2)	5.13	5.07	4.83	4.40	0.65
H–C(1)	5.77	5.71	5.41	4.85	0.92

^a) Estimated average values.

^b) Signal overlap.

^c) Coalescence.

shift is dependent upon the amount of BPh_4^- . Schiemenz ascribed it to ion association of the cation with the BPh_4^- counterion [7], which induces upfield shifts of 1 to 3 ppm of the H–C(α) signals of ammonium or phosphonium tetraphenylborates (α to onium center) with respect to the corresponding halogenides. β - and γ -Protons are less affected (*ca.* 20%). The shift decreases when the approach of the anion is sterically hindered. In this context, it is notable that the allylic protons *cis* to the phosphine moiety demonstrate a rather small shift with respect to the protons *cis* to the dihydrooxazole ring suggesting that the bulky phosphine group prevents a close association at this side of the cation.

Conclusion. – X-Ray analyses show that the conformation of the phosphinoxazole ligand is hardly affected by its environment. The minor changes are due to lattice forces rather than to the properties of the anion. In this work, we found that in the solid state, the $[\text{Pd}^{\text{II}}(\eta^3\text{-allyl})]$ moiety could adopt several configurations between a nearly symmetrical three-electron $\text{Pd}(\pi\text{-allyl})$ system and an asymmetrical allyl group with a η^1 - and a

η^2 -bonding to the metal center. Both configurations of the $[\text{Pd}^{\text{II}}(\eta^3\text{-allyl})]$ system are described in the literature [2][3][5][6]. X-Ray data of **2** and **3** suggest that the 'exo' isomers of the BPh_4^- salts may be closer packed in the lattice than 'endo' isomers. On the other hand, $^1\text{H-NMR}$ results indicate that the 'endo' species predominates in solution. The BPh_4^- ion is a quite effective NMR chemical-shift reagent towards the $(\eta^3\text{-allyl})\{2\text{-}[2'\text{-}(\text{diphenylphosphino})\text{phenyl}]\text{-4,5-dihydrooxazole}\}$ palladium(II) cation. However, its application is limited by the instability of the BPh_4^- salts in CDCl_3 solution. Further investigations with more stable anions containing aromatic groups, e.g. $\text{CH}_3\text{-C}_6\text{H}_4\text{-SO}_3^-$, are planned.

The support of this project by the *Swiss National Science Foundation* (project No. 21-45, 276.95) is gratefully acknowledged.

Experimental Part

General. All solvents were distilled before use. L-Phenylglycinol: *Fluka purum*. NMR Spectra: recorded at r.t. in CDCl_3 on a *Varian-Gemini 300*; ^1H , 300 MHz, chemical shifts δ vs. SiMe_4 (= 0 ppm), coupling constants J in Hz; ^{31}P , 121 MHz, triphenyl phosphate as external reference (–18.0 ppm).

(*S*)-2-[2'-(*Diphenylphosphino*)phenyl]-4,5-dihydro-4-phenyloxazole (**5**) was prepared as described in [8] using 2-(diphenylphosphino)benzotrile (0.91 g, 3.16 mmol), (*S*)-2-amino-2-phenylethanol (0.52 g, 3.75 mmol), and ZnCl_2 (0.50 g, 3.75 mmol). Yield of intermediate Zn compound, 1.288 g (74.9%). Yield of **5**, 0.623 g (64.5%). $^1\text{H-NMR}$ (300 MHz, CDCl_3): 3.93 (*dd*, $J \approx 9.0$, 8.3, 1 H–C(5)); 4.55 (*dd*, $J = 10.1$, 8.3, 1 H–C(5)); 5.22 (*dd*, $J \approx 10.1$, 9.0, H–C(4)); 7.11 (*m*, 1 arom. H); 6.86–6.96 (*m*, 3 arom. H); 7.14–7.22 (*m*, 3 arom. H); 7.24–7.41 (*m*, 12 arom. H); 8.00 (*ddd*, $J = 7.5$, 3.6, 1.5, 1 arom. H). $^{31}\text{P-NMR}$: –5.7.

(\pm)-2-[2'-(*Diphenylphosphino*)phenyl]-4,5-dihydro-4-phenyloxazole (*rac*-**5**) was prepared as described for **5**, with (diphenylphosphino)benzotrile (0.8 g, 2.44 mmol), (\pm)-2-amino-2-phenylethanol (0.50 g, 3.16 mmol), and ZnCl_2 (0.49 g, 3.16 mmol). Yield of intermediate Zn compound, 1.05 g (79.1%). Yield of *rac*-**5** 0.70 g (93.0%). $^1\text{H-NMR}$ (300 MHz, CDCl_3): see **5**.

(η^3 -Allyl){(*4S*)-2-[2'-(*Diphenylphosphino*)phenyl]-4,5-dihydro-4-phenyloxazole}palladium(II) Hexafluorophosphate (**1**). To a soln. of **5** (101 mg, 0.25 mmol) in *i*-PrOH (15 ml) was added under N_2 [$\text{Pd}(\eta^3\text{-C}_3\text{H}_5)\text{Cl}_2$] (46 mg, 0.125 mmol). The suspension was stirred for 1 h at r.t. The clear pale yellow soln. was treated with NH_4PF_6 (100 mg, 0.61 mmol) and stirred for further 20 min. The yield of white solid was 123 mg (70.3%). $^1\text{H-NMR}$ (300 MHz, CDCl_3 , 25°; for numbering, see *Fig. 1*¹): major isomer: 2.64 (*d*, $J = 12.09$, $\text{H}_f\text{-C}(100)$); 2.85 (*dd*, $J = 13.67$, 10.21, $\text{H}_f\text{-C}(300)$); 3.18 (*d*, $J = 6.32$, $\text{H}_e\text{-C}(100)$); 4.29 (*t*, $J \approx 7.69$, 8.83, $\text{H}_1\text{-C}(2)$); 4.77 (*m*, $\text{H}_e\text{-C}(300)$); 5.13 (*dd*, $J = 8.83$, 10.54, $\text{H}_2\text{-C}(2)$); 5.62 (*m*, $\text{H-C}(200)$); 5.77 (*dd*, $J = 7.69$, 10.54, $\text{H-C}(1)$); 6.77–7.75 (*m*, 18 arom. H); 8.25–8.27 (*m*, 1 arom. H); minor isomer: 2.71 (*d*, $J = 12.37$, $\text{H}_f\text{-C}(100)$); 3.31 (*d*, $J = 6.11$, $\text{H}_e\text{-C}(100)$); 4.29 (*t*, $J \approx 7.69$, 8.83, $\text{H}_1\text{-C}(2)$); 3.90 (*dd*, $J = 13.3$, 9.9, $\text{H}_f\text{-C}(300)$); 4.49 (*m*, $\text{H}_e\text{-C}(300)$); 5.13 (*dd*, $J = 8.83$, 10.54, $\text{H}_2\text{-C}(2)$); 5.15 (*m*, $\text{H-C}(200)$); 5.77 (*dd*, $J = 7.69$, 10.54, $\text{H-C}(1)$); 6.77–7.75 (*m*, 18 arom. H); 8.25–8.27 (*m*, 1 arom. H).

(η^3 -Allyl){(\pm)-2-[2'-(*Diphenylphosphino*)phenyl]-4,5-dihydro-4-phenyloxazole}palladium(II) Hexafluorophosphate (*rac*-**1**). As described for **1**, using *rac*-**5** (113.3 mg, 0.28 mmol) and [$\text{Pd}(\eta^3\text{-C}_3\text{H}_5)\text{Cl}_2$] (93.2 mg, 0.14 mmol). Yield 191.4 mg (80.8%). Recrystallization from EtOH/MeCN/Et₂O afforded crystals suitable for X-ray analysis.

(η^3 -Allyl){(*4S*)-2-[2'-(*Diphenylphosphino*)phenyl]-4,5-dihydro-4-phenyloxazole}palladium(II) Tetraphenylborate (**2**). A mixture of [$\text{Pd}(\eta^3\text{-C}_3\text{H}_5)\text{Cl}_2$] (46 mg, 0.25 mmol) and **5** (0.101 mg, 0.25 mmol) was stirred under N_2 in *i*-PrOH (20 ml) for 30 min. The resulting pale yellow solution was treated with NaBPh_4 (100 mg, 0.29 mmol). The inorg. salts were removed with H_2O (20 ml). The residue was dissolved in EtOH/hexane 1:1. Allowing the soln. to stand in a hexane atmosphere for 24 h yielded colorless **2** (200.5 mg, 91.7%). Recrystallization from AcOEt/ CHCl_3 10:1 afforded airstable crystals suitable for X-ray analysis. $^1\text{H-NMR}$ (300 MHz, CDCl_3 , 25°; for numbering, see *Fig. 2*¹): 2.7–2.9 (*br.*, $\text{H}_f\text{-C}(100)$, $\text{H}_e\text{-C}(100)$, $\text{H}_f\text{-C}(300)$); 3.96 (*dd*, $J = 9.09$, 7.95, $\text{H}_1\text{-C}(2)$); 4.17 (*dd*(*t*), $J = 6.76$, $\text{H}_e\text{-C}(300)$); 4.40 (*dd*, $J = 9.07$, 10.37, $\text{H}_2\text{-C}(2)$); 4.85 (*dd*, $J = 7.95$, 10.37, $\text{H-C}(1)$); 5.11 (*m*, $\text{H-C}(200)$); 6.61 (*d*, $J = 7.38$, 2 arom. H); 6.83 (*t*, $J = 7.14$, 4 arom. H); 6.97–7.71 (*m*, 40 arom. H); 8.25–8.27 (*m*, 1 arom. H).

rac-(η^3 -Allyl){2-[2'-(*Diphenylphosphino*)phenyl]-4,5-dihydro-4-phenyloxazole}palladium(II) Tetraphenylborate (*rac*-**2**). A mixture of 46 mg of [$\text{Pd}(\eta^3\text{-C}_3\text{H}_5)\text{Cl}_2$] (0.125 mmol) and of 0.101 mg of *rac*-**5** (0.25 mmol) was

stirred under N₂ in *i*-PrOH (20 ml) for 30 min. The resulting pale yellow soln. was treated with 100 mg of NaBPh₄ (100 mg, 0.29 mmol). The residue was dissolved in CHCl₃, and the inorg. salts were filtered off. Allowing the filtrate to stand in a hexane atmosphere for 24 h yielded colorless *rac*-2 (172 mg, 78.7%). Recrystallization from hexane/CH₂Cl₂ 10:1 afforded airstable crystals suitable for X-ray analysis.

(η^3 -Allyl)₃(4*S*)-2-[2'-(Diphenylphosphino)phenyl]-4,5-dihydro-4-isopropylloxazole}palladium(II) Tetraphenylborate (3). A mixture of [Pd(η^3 -C₃H₅)Cl]₂ (44 mg, 0.12 mmol) and (4*S*)-2-[2'-(diphenylphosphino)phenyl]-4,5-dihydro-4-isopropylloxazole (84 mg, 0.22 mmol) was stirred under N₂ in *i*-PrOH (20 ml) for 1 h. The clear soln. was treated with NaBPh₄ (98 mg, 0.29 mmol). After 2 min, the brownish precipitate was collected and dissolved in CHCl₃. The inorg. salts were filtered off. Adding hexane to the filtrate yielded colorless 3 (172 mg, 90.0%). Recrystallizing in EtOH/hexane/CHCl₃ 3:3:1 afforded airstable crystals suitable for X-ray analysis. ¹H-NMR (300 MHz, CDCl₃, 25°; for numbering, see Fig. 4)¹: 0.12 (*d*, *J* = 6.9, 1 Me); 0.68 (*d*, *J* = 7.1, 1 Me); 1.71 (*m*, H–C(400)); 2.82 (*br. d*, H₁–C(100)); 3.15 (*br. d*, H₂–C(100)); 3.31 (*dd*, *J* = 10.2, 13.7, H₁–C(300)); 3.90 (*dt*, *J* = 7.8, 3.2, H–C(1)); 4.08 (*d*, *J* = 7.8, 2 H–C(2)); 4.35 (*t*, *J* ≈ 6.6, H₃^b–C(300)); 5.41 (*m*, H–C(200)); 6.80–7.66 (*m*, 33 arom. H); 8.15–8.19 (*m*, 1 arom. H).

X-Ray Structure Analyses. Crystal data and parameters of the data collection are compiled in Table 4. Unit-cell parameters were determined by accurate centering of 25 strong reflections. Reflection intensities were

Table 4. Experimental Conditions for the X-Ray Analysis of Compounds 1, 2, *rac*-2, and 3

	<i>rac</i> -1	2	<i>rac</i> -2	3
Molecular formula	C ₃₀ H ₂₇ F ₆ NOP ₂ Pd · (C ₂ H ₆ O) _{0.5}	C ₅₄ H ₄₇ BNOPPd	C ₅₄ H ₄₇ BNOPPd	C ₅₁ H ₄₉ BNOPPd
Molecular weight	722.9	874.16	874.16	840.14
Crystal system	monoclinic	monoclinic	monoclinic	monoclinic
Space group	<i>P</i> 2 ₁ / <i>c</i>	<i>P</i> 2 ₁	<i>P</i> 2 ₁ / <i>c</i>	<i>P</i> 2 ₁
<i>a</i> [Å]	9.752(1)	9.781(1)	10.339(2)	10.931(1)
<i>b</i> [Å]	17.036(3)	15.886(4)	17.184(1)	14.520(1)
<i>c</i> [Å]	18.545(3)	15.048(1)	24.854(6)	13.538(1)
β [°]	92.35(1)	108.36(1)	100.36(2)	97.56(4)
<i>V</i> [Å ³]	3078.2(9)	2219.4(7)	4343.7(1.5)	2130.0(2)
Calc. density [g/cm ³]	1.567	1.308	1.337	1.31
Crystal size [mm]	0.20 × 0.24 × 0.41	0.14 × 0.18 × 0.42	0.15 × 0.42 × 0.75	0.14 × 0.14 × 0.42
<i>Z</i>	4	2	4	2
Temp. [K]	293	293	293	293
Radiation	MoK _α (λ = 0.71069 Å)	CuK _α (λ = 1.54180 Å)	CuK _α (λ = 1.54180 Å)	CuK _α (λ = 1.54180 Å)
<i>F</i> (000)	1460	904	1808	872
Abs. coeff. [cm ⁻¹]	7.6	11.4	11.7	11.7
θ_{\max} [°]	30.44	77.50	77.50	77.50
Scan type	$\omega/2\theta$	$\omega/2\theta$	$\omega/2\theta$	$\omega/2\theta$
No. of meas. refl.	6997	4205	8686	4570
No. of obs. refl.	6721	4054	8331	4347
No. of refl. in ref. <i>I</i> ≥ 3 σ (<i>I</i>)	4011	3572	7333	3960
No. of parameters	503	554	592	526
Extinction parameter		73.8(9.1)	94.4(6.3)	
Standards decay [%]	7.80	3.23	9.03	20.18
Absorption correction				
min, max	1.16, 1.23	1.16, 1.46	1.15, 2.43	1.16, 1.32
Goodness of fit	1.1002	1.0418	0.9622	1.0397
Final Δ_{\max}/σ	0.354	0.437	0.275	0.526
$\Delta\rho$ (min, max) [eÅ ⁻³]	–0.34, 0.42	–0.93, 0.87	–1.44, 1.06	–0.52, 0.61
Final <i>R</i>	3.90	4.55	5.26	3.68
Final <i>R</i> _w	4.02	5.07	6.61	3.97
Weighting scheme	<i>Chebyshev</i> weighting scheme [12]			

collected on a four-circle diffractometer (*Enraf-Nonius CAD4*). Three standard reflections were monitored every hour during data collection. The usual corrections were applied. The structures were solved by direct methods [9]. Anisotropic least-squares refinement on F was carried out on all non-H-atoms using the program CRYSTALS [10]. Isotropic refinement was carried out on all allylic protons. The C–H distances were fixed to 0.96 Å, the corresponding H–C–H, C–C–H and Pd–C–H angles were restrained to their mean value. Positions of the remaining H-atoms were calculated. Scattering factors were taken from the 'International Tables of Crystallography, Vol. IV.' *Figs. 1–4* were designed with the programme SNOOPI [11]. The allyl ligand of *rac-1* and *rac-2* was found to be disordered and refined with all atoms in two positions. Occupancy factors were refined for the 'exo' and 'endo' orientations, resp., holding the sum of their occupancies equal to 1. The final values were 0.49(2) and 0.51 for *rac-1* and 0.65(1) and 0.35 for *rac-2*. In *rac-1*, corresponding Pd–C and C–C bond lengths of the two diastereoisomers were restrained to their mean value with e.s.d.s of 0.01. The C–C–C angles were restrained to their mean value with an e.s.d. of 4.0. In *rac-1*, the F-atoms of the disordered PF_6^- anion were refined in two positions. Restraints for an ideal octahedral geometry were applied.

REFERENCES

- [1] a) P. von Matt, A. Pfaltz, *Angew. Chem.* **1993**, *105*, 614; *ibid. Int. Ed.* **1993**, *32*, 566; b) P. von Matt, Ph.D. Thesis, University of Basel, 1993; c) J. Sprinz, G. Helmchen, *Tetrahedron Lett.* **1993**, *34*, 1769; d) G. I. Dawson, C. G. Frost, J. M. J. Williams, S. J. Coote, *ibid.* **1993**, *34*, 3149.
- [2] a) J. Sprinz, M. Kiefer, G. Helmchen, M. Reggelin, G. Huttner, O. Walter, L. Zsolnay, *Tetrahedron Lett.* **1994**, *35*, 1523; b) B. Hofmann, work performed in the 'anorganisch-chemisches Fortgeschrittenenpraktikum' of the RWTH Aachen in the group of M. Zehnder, Universität Basel, 1993; c) L. Macko, Ph.D. Thesis, University of Basel, 1996.
- [3] N. Baltzer, L. Macko, S. Schaffner, M. Zehnder, *Helv. Chim. Acta* **1996**, *79*, 803.
- [4] M. Dobler, 'ColorMoMo 1.4', ETH Zurich, 1994.
- [5] G. J. P. Britovsek, W. Keim, S. Mecking, D. Sainz, T. Wagner, *J. Chem. Soc., Chem. Commun.* **1993**, 1632.
- [6] M. C. Bonnet, S. Agbossou, I. Tkatchenko, R. Faure, H. Loiseau, *Acta Crystallogr., Sect. C: Cryst. Struct. Commun.* **1987**, *43*, 445.
- [7] G. P. Schiemenz, *J. Magn. Reson.* **1972**, *6*, 291; G. P. Schiemenz, *Tetrahedron* **1973**, *29*, 741; G. P. Schiemenz, H. P. Hansen, *Angew. Chem.* **1973**, *85*, 404; G. P. Schiemenz, *J. Organomet. Chem.* **1973**, *52*, 349.
- [8] G. Koch, G. Lloyd-Jones, O. Loiseau, A. Pfaltz, R. Prétôt, S. Schaffner, P. Schnyder, P. von Matt, *Recl. Trav. Chim. Pays-Bas* **1995**, *114*, 206.
- [9] A. Altomare, M. C. Burla, M. Camalli, G. Cascarano, C. Giacovazzo, A. Gualgiardi, G. Polidori, 'SIR92', *J. Appl. Crystallogr.* **1994**, *27*, 435.
- [10] D. Watkin, 'Crystals, Issue 9', Chemical Crystallography Laboratory, Oxford, 1990.
- [11] K. Davies, P. Braid, B. Foxman, H. Powell, 'SNOOPI', Oxford University, 1989.
- [12] J. R. Carruthers, D. J. Watkin, *Acta Crystallogr., Sect. A* **1979**, *35*, 689.